Traffic & Transportation

Research on Two-Stage Pedestrian Crossing Inductive Signal Control Strategy for Autonomous Intersection

Qianyi ZHANG[1], Xinrui YU[2], Yugang LIU[3], Liying TANG[4]

Original Scientific Paper
Submitted: 16 Sep 2024
Accepted: 23 Dec 2024

[1] zhangqianyi@my.swjtu.edu.cn, School of Transportation and Logistics, Southwest Jiaotong University, Chengdu, China
[2] yuxinrui@my.swjtu.edu.cn, School of Transportation and Logistics, Southwest Jiaotong University, Chengdu, China
[3] Corresponding author, liuyugang@swjtu.edu.cn, School of Transportation and Logistics, Southwest Jiaotong University, Chengdu, China
[4] tly2014112724@163.com, Department of Road Traffic Management, Sichuan Police College, Luzhou, China

Publisher:
Faculty of Transport and Traffic Sciences, University of Zagreb

ABSTRACT
Autonomous intersection management (AIM) at "signal-free" intersections under the fully Connected-Automated Vehicle (CAV) environment has become a hotspot. However, few studies show how pedestrians can cross the intersection safely with CAVs. This paper proposes a novel inductive signal control framework considering both pedestrian and CAV demands. This framework consists of two steps. In the first step, a two-stage pedestrian crossing inductive control module for autonomous signal intersections is implemented. In the second step, the CAVs' trajectories and pedestrian crossing phases are optimised cooperatively. A Mixed Integer Linear Program (MILP) based on conflict-separation is proposed to simultaneously optimise the pedestrian crossing signal phasing scheme and the entry time for CAVs. The goal is to ensure pedestrian crossing safely while optimizing the approaching trajectories of CAVs at the intersection. Numerical experiments are conducted to evaluate the performance and effectiveness of the proposed method under different traffic scenarios. Results show that the proposed method outperforms the signal control mode for pedestrian crossing in one go in terms of reducing average delay under both under-saturated and over-saturated conditions.

KEYWORDS
autonomous intersection management; connected-automated vehicles; pedestrian crossing; mixed integer linear program.

1. INTRODUCTION

The rapid development of intelligent transportation technology has indeed sparked significant interest among researchers regarding autonomous intersection management (AIM) models. With AIM, the elimination of physical traffic signals represents a transformative shift in how intersections are managed. Once Connected-Automated Vehicles (CAVs) enter the communication range of the intersection, they will exchange information by communicating in real-time with surrounding vehicles (V2V) or roadside infrastructure (V2I). Therefore, the driving strategies of CAVs can be optimised by the central controller of the intersection. Compared with the signal control method, this method will effectively improve the efficiency of spatial and temporal resource utilization and capacity of the intersection and will perform better in terms of efficiency, energy consumption and safety.

AIM can be divided into rule-based reservation methods and optimization-based methods. Among the rule-based reservation methods, Dresner et al. [1] gave an early model of autonomous intersection vehicle movements in 2008. The model used a first-come-first-served (FCFS) intersection control strategy, where all autonomous vehicles requested intersection right-of-way based on the chronological order of their arrivals at

the intersection. The results showed that the model was able to reduce delays compared to signal control methods. Li et al. [2] constructed four algorithms to plan the trajectories of CAVs inside intersections based on a safe driving model using the spanning tree method. Ahmane et al. [3] constructed an autonomous intersection control strategy via Petri nets and proved the model's validity by comparing it with the FCFS strategy. According to the value of time for different travellers, Carlino et al. [4] considered multiple factors, such as driver characteristics and distance to the destination, to grant rights of way to high-priority CAVs through competition rules. In addition, they also studied the social equity issues implied by the bidding for CAVs. Chen et al. [5] proposed a novel intersection design called knotted intersection (KI) to resolve the complexity of conflicting relations at intersections in a full CAV environment. They also developed Rhythm Control (RC) rules for the KI, which were derived to have properties including nearly throughput-maximizing and ensuring bounded within-intersection delay for vehicles.

Other scholars have focused their research on optimization-based methods. Lee et al. [6] used the basic idea of air control theory to construct a vehicle movement model at intersections to minimise the conflict distance. Zhu et al. [7] developed a lane-based two-layer optimization model that considered dynamic departure time, dynamic route choice, and autonomous intersection control in the context of a system optimum network model to propagate traffic flows and then transformed it into a linear programming formulation for autonomous intersection control (LPAIC). Muller et al. [8] transformed the autonomous intersection control problem into three more detailed control subproblems using a Mixed Integer Linear Programming (MILP) model to minimise vehicle delay. They were the computation of feasible arrival times for each vehicle, the scheduling problem of vehicle arrival time at the intersection, and the motion planning problem for vehicles to reach the intersection at the scheduled time. Levin et al. [9] used the MILP model to coordinate the passing time of CAVs at conflict points under AIM* and proposed a rolling-horizon algorithm to enlarge the scale of model solving. Fayazi et al. [10] similarly constructed a MILP-based control model for autonomous intersections to optimise car arrival times and travel speeds at intersections based on an intelligent grid environment. Lu et al. [11] designed three intersection control strategies: a signal-free strategy, a signal-free strategy considering safety buffers and a signal-based strategy. Numerical experiments were conducted to compare the traffic efficiency of vehicles under each strategy. It was found that the control efficiency of the signal-free strategy was significantly better than that of the signal-based strategy. The optimal solution of the signal-free strategy with safety buffers then tends to generate groups of vehicles and release them in turn at the intersection. Chen et al. [12] proposed a controllable gap strategy for the central controller considering the conflict relationship. This strategy presented a rapid check criterion for conflict-free time slots in the conflict set of the reservation to avoid a potential collision, which removes unnecessary judgments. Deng et al. [13] presented a Vehicle-Platoon-Aware Bi-Level Optimization Algorithm for Autonomous Intersection Management (VPA-AIM) to coordinate the merging of CAVs at unsignalised intersections. Hao et al. [14] also proposed a MILP model to optimise vehicle trajectories at an isolated "signal-free" intersection without lane allocation, denoted as "lane-allocation-free" (LAF) control. In this way, lanes are no longer restricted to specific directions, so the spatial-temporal resources are fully utilised. Furthermore, Mahdi et al. [15] aimed to minimise the total crossing time, as well as the energy consumption due to the acceleration of CAVs. The intersection lane-free crossing problem is formulated as a multi-objective Optimal Control Problem (OCP) with constraints to avoid vehicle-to-vehicle collisions and vehicle-to-boundary collisions. Convex optimization duality theory is applied to smooth the problem, ultimately generating lane-free trajectories for vehicles. Hua et al. [16] incorporated ethical and social factors into the cooperative trajectory planning of CAVs passing through intersections, making it more aligned with the demands and challenges of the real world.

It is worth noting that most of the existing studies on AIM models assume that road users are only motorised vehicles, ignoring the presence of pedestrians. Such assumptions do not correspond to realistic traffic scenarios and hinder the practical application of AIM methods.

Pedestrian crossings at intersections include two types. The first type is an uncontrolled pedestrian crossing. Pedestrians can directly go through crosswalks according to a crossable time gap after observing. This type of crossing is usually applied when vehicle or pedestrian crossing demands are small. When the intersection size is large and the crossing distance is long, it is not possible to complete the crossing in one crossable time gap. A refuge island is usually set to provide a temporary safe waiting area for pedestrians in the middle of crosswalks, using existing space such as the central divider and green belt. The second type is a control-based pedestrian crossing, which separates pedestrian flows with conflicting vehicle flows temporally with signal control. The advantage of control-based pedestrian crossing is that the signals improve pedestrian crossing safety by completely separating conflicts [17].

Pedestrian signal control methods mainly include fixed timing signal control and inductive signal control. Fixed timing signal control is relatively simple and usually refers to the setting of fixed and reasonable pedestrian crossing phases in advance to ensure a stable passage time for pedestrians. Based on scientific detection technology, such as coil detectors and video recognition technology, inductive signal control collects real-time information on vehicle and pedestrian flows. Then, signal control parameters are adjusted to enhance intersection efficiency. Compared with fixed timing signal control, the flexible phase switching and parameter configuration of the inductive signal control method are more adaptable to random traffic flows. The idle time of the green phase is effectively reduced, and thus redundant occupation of intersection right-of-way by pedestrians is reduced.

In recent years, some scholars have explored how to rationally design pedestrian crossing strategies under AIM models. Gupta et al. [18] first conceptualised the vehicle-pedestrian negotiation process by proposing a framework for negotiating the priority of access between pedestrians and self-driving vehicles. Niels et al. [19] proposed an intersection management scheme that incorporates pedestrian signals into the FCFS-based AIM framework and put forward two strategies: fixed-cycle pedestrian signal control and pedestrian inductive signal control. The fixed-cycle strategy provided pedestrians with the full right-of-way. Under pedestrian inductive signal control, pedestrians trigger a crossing request. The findings show that a pedestrian-actuated signal control strategy delivers better performance than fixed-cycle signal control. Chen et al. [20] developed an optimisation model called AIM-ped to balance the right-of-way allocation between pedestrians and vehicles. Specifically, pedestrian crossings are facilitated with pedestrian-specific activation signals. When the pedestrian crossing is activated, the conflicting vehicles are prohibited from crossing the intersection. However, AIM-ped may reduce intersection capacity due to blockages resulting from conflicts between vehicle lanes and crosswalks. El Hamdani et al. [21] proposed an autonomous pedestrian crossing system (APC) for signal-free intersections. The APC defines a set of crossing rules, relocating the crosswalk from within the intersection to a section of the road some distance away from the intersection. The pedestrian crossing is completely separated. However, high pedestrian crossing demands may result in traffic bottlenecks or even vehicle flow disruption. Niels et al. [22] and Cai et al. [23] are among the earliest to consider pedestrians in optimisation-based AIM. They proposed methods that integrate unsignalised vehicle control with pedestrian signalling for centralised optimisation. The proposed cooperative strategies not only balanced the benefits of vehicles and pedestrians but also improved the traffic efficiency at the intersection. Mokhtari and Wagner [24], [25] proposed a deep reinforcement learning method that enabled autonomous vehicles to safely interact with pedestrians at unsignalised intersections and further compared the performance of different deep reinforcement learning methods trained on their reward function and state representation. Malcolm P et al. [26] proposed an innovative lane-free autonomous intersection management algorithm based on the "first-come, first-served" principle, specifically designed for urban environments, with priority given to vulnerable road users (such as pedestrians and cyclists). Simulation results show that this method provides high-quality service to vulnerable road users while also improving the traffic efficiency of connected autonomous vehicles.

Wu et al. [27] made the first attempt to solve the pedestrian crossing problem at autonomous intersections using an automated pedestrian shuttle (APS) system. Discrete pedestrian crossing behaviours are transformed into deterministic behaviours as the APS vehicle can carry pedestrians to pass through the intersection. A capability-based model was proposed to calculate and coordinate the crossing schedules between AVs and APSs. Based on that, Jiang et al. [28] constructed an APS path optimisation model. The model further optimised the APS order and the duration of its stops. However, the multiple fixed APS paths may result in a significant increase in conflicts within the intersection. Particularly, when the pedestrian crossing demand is high, the use of APS crossings may result in long waiting times for pedestrians due to the capacity constraints of APS vehicles. In addition, the APS method requires pedestrians to get on and off, which may result in discomfort and a poor travelling experience for pedestrians. Compared with the APS crossing, the pedestrian inductive signal control method is in line with pedestrian travel habits and can accommodate the randomness of pedestrian movements. Moreover, the inductive signal control method is better suited for scenarios with high pedestrian demands as it allows more pedestrians.

To address the current limitations, this paper innovatively proposes a two-stage pedestrian crossing inductive signal control (PCISC) method. A conflict occupancy-based trajectory planning model for CAVs is also proposed to realise the safe crossing of vehicles and pedestrians. The PCISC system can send a green phase release request to the central controller based on real-time pedestrian arrivals. The central controller then optimises the overall signal timing by considering the current vehicle status within the intersection, vehicle passing requests and the green phase release request. This approach allows the system to select an appropriate

time gap to release pedestrians while minimizing vehicle passing time at the intersection, thus improving the overall efficiency.

The remainder of this article is structured as follows. Section 2 describes the intersection scenarios and modelling assumptions. Section 3 presents the PCISC strategy. Section 4 proposes a co-optimisation model for the central controller at intersections based on collision avoidance. Section 5 implements numerical analysis and evaluates the model's validity. Finally, the work is summarised in Section 6.

2. PROBLEM DESCRIPTION

2.1 Intersection layout

A conventional four-arm intersection is taken as an example in this paper. The intersection area consists of the optimisation area and the inner area as shown in *Figure 1*. Pedestrian crosswalks are located before the stop lines at each of the approaches, and pedestrian refuge islands for two-stage crossing are set at the centre line of the approaches. Pedestrian waiting areas are located at the four corners of the intersection, with pedestrian crossing request buttons or video detectors installed roadside to detect pedestrian crossing needs. Traffic signals are set at the roadsides of the intersection and refuge islands. Additionally, smart crosswalk physical barriers are introduced. These barriers allow pedestrians to cross when the signal switches to the green phase. Otherwise, it will prohibit pedestrians from crossing during the red phase.

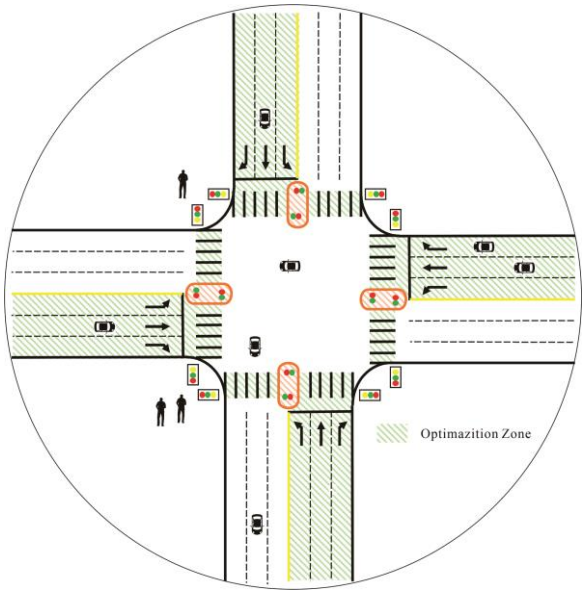

Figure 1 – Intersection layout with two-stage PCISC

2.2 Intersection control logic

In the PCISC system, the following rules for vehicle and pedestrian movements at intersections are set up:

The vehicle first enters the intersection communication zone and requests the central controller. When the entering request is accepted, it should follow the message fed back from the central controller to pass the optimisation zone. The message specifies the passing time at the stop line, which is the entry time at the intersection. Then, the vehicle maintains the maximum speed to pass the inner area of the intersection.

After the central controller detects the pedestrian crossing demand, the two-stage crossing signal timing will be generated according to the optimisation model and fed back to the signal lights. Pedestrians complete the first stage crossing according to the roadside signal instructions and the second stage crossing according to the refuge island signal instructions.

The information transfer logic is as follows. When a vehicle enters the optimisation area, it sends a passing request to the central controller with its current position, speed, arrival time and acceleration/deceleration information. At the same time, the central controller continuously detects information about the emergence time and number of pedestrians at the roadside. Subsequently, the travel strategy of the requesting vehicle and the pedestrian signal timing strategy are calculated via the cooperative optimisation model and are sent back to the vehicle and the signal.

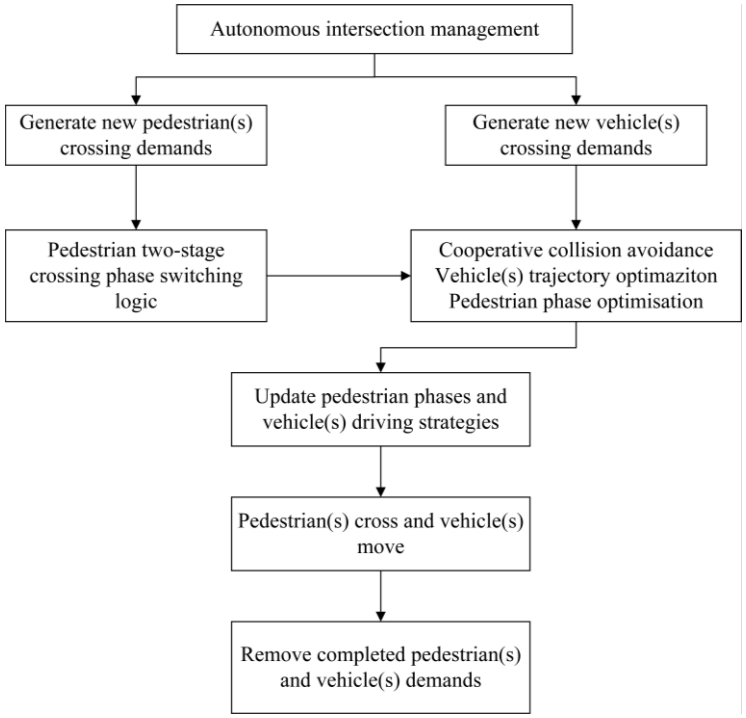

Figure 2 – Intersection control logic

2.3 Model notations and assumptions

In this paper, assumptions are made as follows:

1) It is assumed that pedestrians cross in full compliance with the signal instructions. Red light running behaviour is not allowed.
2) Pedestrians can complete the crossing once they enter the intersection, and no pedestrians are left for the next releasing phase.
3) The roadside waiting area and the refuge island have enough space to accommodate all crossing pedestrians.
4) Vehicle paths are known and fixed before entering the intersection.
5) The diversion or merging conflicts within the intersection are not considered.
6) The delay of V2V and V2I communications is not considered.

Table 1 – Notations and definitions

Notation	Definition
C	Set of vehicle demands
P	Set of pedestrian crossing demands
R^P	Set of pedestrian crossing paths
R^C	Set of paths chosen by the vehicle
q_0^p	The initial volume of pedestrians
$r_{i,j}^p$	Path number of pedestrian crossing, where $i, j \in \{a, b, c\}$
t_{p_i}	Critical safety gap(s) required for safe pedestrian crossing, $i = 0$ denotes the pedestrian crossing path of the first stage $r_{a,c}^p$; $i = 1$ denotes the pedestrian crossing path of the second stage $r_{c,b}^p$
$t_{p_i}^-$	$i = 0$ denotes the time(s) when pedestrian crossing demand occurs at the initial waiting area a; $i = 1$ denotes the time(s) when pedestrians safely cross the first stage crossing path $r_{a,c}^p$ and reach the refuge island c before the second stage crossing
t'_{p_i}	$i = 0$ denotes the phase release time (s) for pedestrians crossing the first stage crossing path $r_{a,c}^p$; $i = 1$ denotes the phase release time (s) for pedestrians crossing the second stage crossing path $r_{c,b}^p$

Notation	Definition
t_p	Pedestrian crossing phase duration (s)
x_t^c	Distance travelled by vehicle c at time t (m)
L_c^r	The total length of vehicle path r^c (m)
L_{adjust}	Length of optimisation zones (m)
ε	Minimal positive numbers
v_m	Vehicle traveling speed inside the intersection (m/s)
v_{c0}	Initial speed of vehicles arriving at the intersection (m/s)
l_c	Vehicle length (m)
a	Marked initial waiting area for pedestrian crossing
c	Pedestrian refuge island
b	Pedestrian crossing destination
t_φ	Maximum tolerable waiting time for pedestrians on the roadside, taken as 30 s
$t_{\varphi'}$	Maximum tolerable waiting time for pedestrians at the refuge island for two-stage crossings, taken as 20 s
t_c^-	The arrival time of the vehicle (s)
t_c'	The optimal time for a vehicle to be allowed to enter an intersection (s)
$\underline{\delta}_c^{b,r}$	The lower location boundary of the conflict area between vehicle paths
$\overline{\delta}_c^{b,r}$	The upper location boundary of the conflict area between vehicle paths
B_r	Set of conflict areas between vehicle paths
$\underline{\mu}_c^{s,r}$	Location of the lower boundary of the conflict area between the vehicle path and the pedestrian crosswalks
$\overline{\mu}_c^{s,r}$	Location of the upper boundary of the conflict area between the vehicle path and the pedestrian crosswalks
S_r	Set of conflict areas between vehicle paths and pedestrian crosswalks
Δd	Safe vehicle following distance (m)
ϑ_{ij}	A binary variable used to determine the relationship between the front and rear positions of vehicles on the same path, $\forall i,j \in C, i \neq j$
$\underline{t}_c^{b,r}$	Arrival time of vehicles at the lower boundary of the conflict zone (s)
$\overline{t}_c^{b,r}$	Arrival time of vehicles at the upper boundary of the conflict zone (s)
$\underline{t}_c^{s,r}$	Arrival time of vehicles at the lower boundary of the conflict zone between the vehicle path and the pedestrian crossing (s)
$\overline{t}_c^{s,r}$	Arrival time of vehicles at the upper boundary of the conflict zone between the vehicle path and the pedestrian crossing (s)
t_c^+	The time of the vehicle leaving the intersection (s)
$y_{c,t}^b$	A binary variable for determining whether a vehicle has entered a conflict zone of B_r
$y_{c,t}'^b$	A binary variable for determining whether a vehicle has left the conflict zone of B_r
$z_{c,t}^s$	A binary variable for determining whether a vehicle has entered the conflict zone of S_r
$z_{c,t}'^s$	A binary variable for determining whether a vehicle has left the conflict zone of S_r
$z_{p,t}^s$	A binary variable for determining whether the pedestrian green phase has released at time t
$z_{p,t}'^s$	A binary variable for determining whether the pedestrian green phase has ended at time t

3. TWO-STAGE PCISC MODEL

3.1 Two-stage pedestrian crossing path

For each approach, define the first pedestrian arrival roadside as a, the destination as b, and the two-stage crossing refuge island as c. The pedestrian path can be expressed as $a - c - b$. Each path is indicated by $r^p = (r^p_{a,c}, r^p_{c,b})$. Signal 1 indicates the crossing of pedestrians on $r^p_{a,c}$, Signal 2 indicates the crossing of pedestrians on $r^p_{c,b}$.

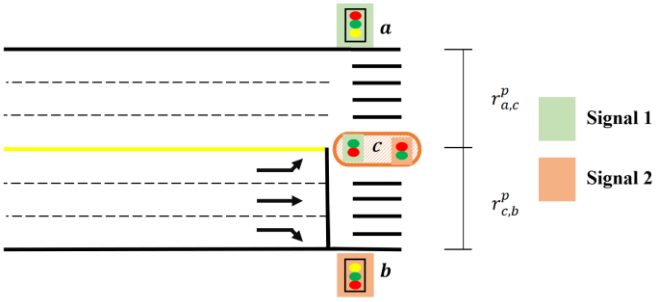

Figure 3 – Schematic diagram of the two-stage crossing path for pedestrians

3.2 Two-stage PCISC model

Each pedestrian p independently has a virtual crossing phase. This phase scheme can be obtained by solving the conflict avoidance model in Section 4. The first second phase start time and second phase start time should be later than the pedestrian arrival time as shown in *Equations 1* and *4*. The difference between the pedestrian phase release time and the pedestrian arrival time should not be greater than the maximum tolerable waiting time as is shown in *Equations 2* and *5*. The pedestrian arrival time at the refuge island equals the sum of the start time of the green phase of the first stage and the minimum pedestrian passing time, as is shown in *Equation 3*.

$$t'_{p_0} \geq t^-_{p_0} \tag{1}$$

$$t'_{p_0} \leq t^-_{p_0} + t_\varphi \tag{2}$$

$$t^-_{p_1} = t'_{p_0} + t_{p_0} \tag{3}$$

$$t'_{p_1} \geq t^-_{p_1} \tag{4}$$

$$t'_{p_1} \leq t^-_{p_1} + t_{\varphi'} \tag{5}$$

According to the HCM manual [29], the occupied length of the pedestrian crosswalk can be obtained by *Equation 6*.

$$L = q \cdot A/d \tag{6}$$

— q – Pedestrian crossing volume;
— d – Width of the pedestrian crosswalk, taken as 3 m;
— A – Average pedestrian footprint, taken as 0.75 m * 0.75 m.

The minimum green time for a pedestrian crossing can be calculated as *Equation 7*, which is determined by the length of the pedestrian crosswalk and the walking speed of the pedestrian.

$$t_{p_0} = (nW + L/v_p) + t_R + t_l \tag{7}$$

— t_{p_0} – Critical crossing gap required for safe pedestrian crossing;
— n – Number of lanes;
— W – Width of the lane, taken as 3 m;
— v_p – Pedestrian walking speed, taken as 1.2 m/s;
— t_R – Reaction time required for pedestrians to cross, taken as 2 s;
— t_l – Time for the vehicle to pass through a crosswalk, $t_l = l_c/v_m$.

One-way pedestrian flow request crossing

For a one-way pedestrian flow ($a-c-b$), the control logic is as follows. Define the time when the pedestrian arrives at the roadside a as $t_{p_0}^-$. The central controller optimises to obtain the green phase start time and duration of the first stage crossing $a-c$ as $[t'_{p_0}, t'_{p_0}+t_{p_0}]$. The arrival time of the pedestrian at the refuge island c is $t_{p_1}^-$. The phase start time and duration of the second stage pedestrian crossing $c-b$ is $[t'_{p_1}, t'_{p_1}+t_{p_1}]$. Then the optimised phases are sent to the pedestrian signals.

Two-way pedestrian flow request crossing

The case involving a two-way pedestrian request to cross ($a-c-b$ and $b-c-a$) is considered. The pedestrians that arrive earlier at roadside a and later at roadside b are denoted as p and p', respectively. The time at which the marked pedestrian p occurs at a is denoted as $t_{p_0}^-$. The time at which the marked pedestrian p' occurs at b is set as $t_{p_0}^-{}'$. The virtual phase schemes of pedestrians p and p' can be obtained by solving the conflict avoidance model in Section 4.

The phase of Signal 1 is determined by two virtual phases: the virtual phase $[t'_{p_0}, t'_{p_0}+t_{p_0}]$ of the first-stage crossing of pedestrian p and the virtual phase $[t'_{p_1}{}', t'_{p_1}{}'+t_{p_1}{}']$ of the second-stage crossing of pedestrian p'. Similarly, the phase of Signal 2 is determined by the virtual phase $[t'_{p_1}, t'_{p_1}+t_{p_1}]$ and the virtual phase $[t'_{p_0}{}', t'_{p_0}{}'+t_{p_0}{}']$. Normally, phases of Signals 1 and Signal 2 can be set directly according to the virtual green phases. However, if the virtual green phases for pedestrian p and pedestrian p' overlap, the phases of Signals 1 and Signal 2 should be set based on the virtual green phases' relationship between pedestrian p and pedestrian p' discussed as follows.

Case 1: If the arrival time of pedestrian p' satisfies the constraint: $t_{p_0}^- \le t_{p_0}^-{}' \le t'_{p_0}+t_{p_0}$ and the virtual green phase release time $t'_{p_0}{}'$ on side b satisfies the constraint: $t'_{p_0}+t_{p_0} \le t'_{p_0}{}' \le t'_{p_1}$, then set the start green time of Signal 2 to be $t'_{p_0}{}'$. The phase duration of Signal 2 is taken as $max(t_{p_1}, t_{p_0}{}')$.

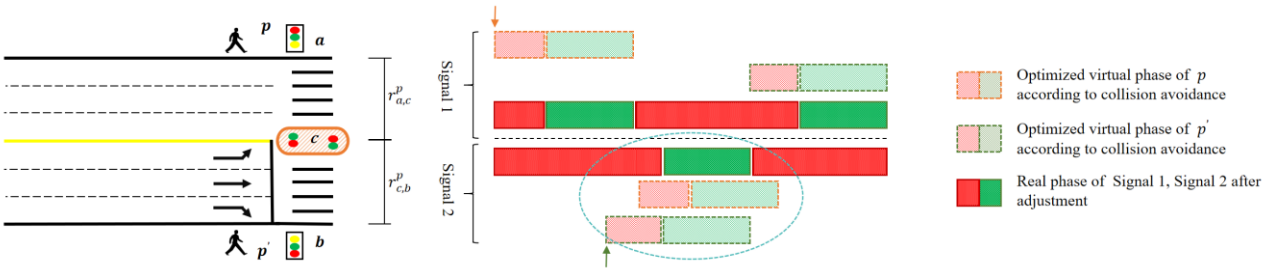

Figure 4 – Two-way pedestrian crossing phase of Case 1

Case 2: If the arrival time of pedestrian p' satisfies the constraint: $t_{p_0}^- \le t_{p_0}^-{}' \le t'_{p_0}+t_{p_0}$ and the virtual green phase release time $t'_{p_0}{}'$ on side b satisfies the constraint: $t'_{p_0}{}' \ge t'_{p_1}$, then set the start green time of Signal 2 to be t'_{p_1}. The phase duration of Signal 2 is taken as $max(t_{p_1}, t_{p_0}{}')$.

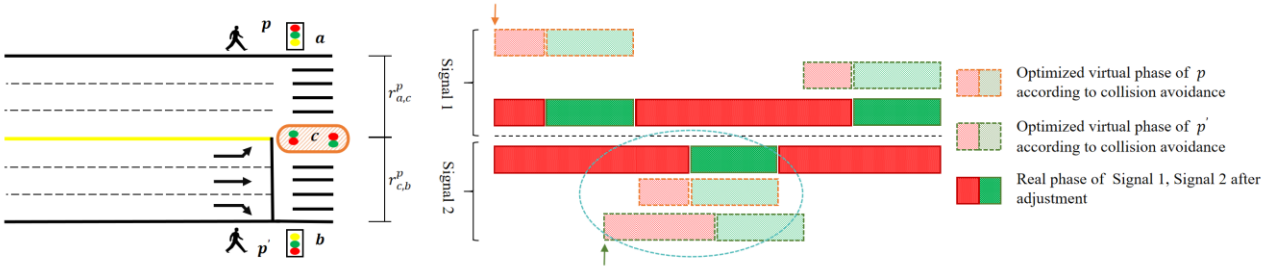

Figure 5 – Two-way pedestrian crossing phase of Case 2

Case 3: If the arrival time of pedestrian p' satisfies the constraint: $t'_{p_0}+t_{p_0} \le t_{p_0}^-{}' \le t'_{p_1}$, then set the real green phase release time of Signal 2 to be t'_{p_1}. The phase duration should be taken as $max(t_{p_1}, t_{p_0}{}')$.

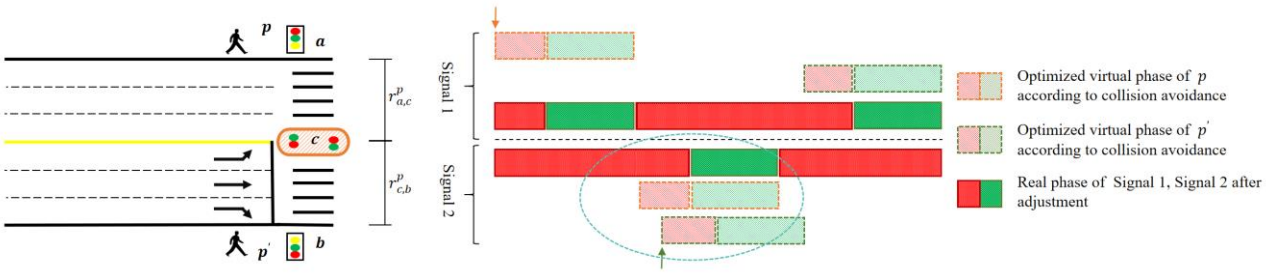

Figure 6 – Two-way pedestrian crossing phase of Case 3

4. COOPERATIVE OPTIMISATION OF CAVs AND PEDESTRIAN CROSSING PHASES

4.1 Modelling of vehicle trajectories and conflict zones

The vehicle is denoted as c and the vehicle set is denoted as C, $c \in C$. A set of vehicle paths is also defined as R^c. Each path r^c represents a distinct route within the intersection, $r^c \in R^c$. The paths are represented by lane boundaries and centerlines, indicated by gray and orange line segments in *Figure 7*. The trajectories for left-turning and right-turning vehicles within the intersection are modelled using elliptical equations. The trajectories for through vehicles are modelled using linear equations. Each path r^c consists of fixed start and end positions, along with a sequence of ordered conflict zones along the path. The path length is denoted as L_{r^c}. The lower and upper boundaries of the conflict zones are represented by $\underline{\delta}_c^{b,r}$, $\overline{\delta}_c^{b,r}$. The set of conflict zones on the path is denoted as B_r. The vehicle length l_c is set as 4 m.

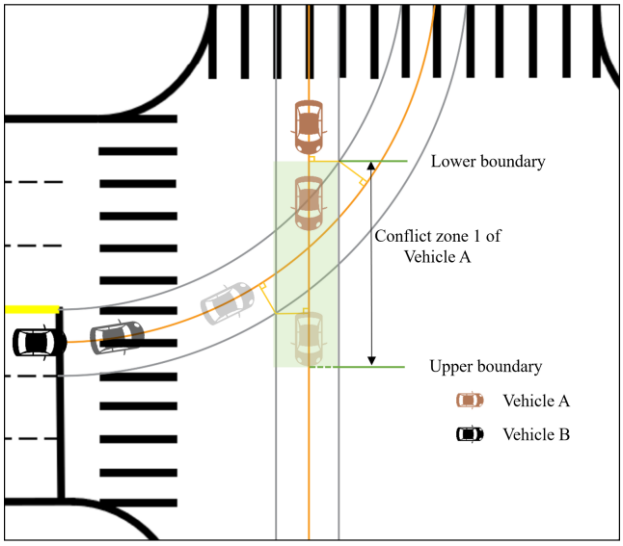

Figure 7 – Vehicle trajectories and conflict zones within the intersection

4.2 Basic constraints

Vehicle following constraints. For vehicle i and vehicle j with the same path, if vehicle j reaches the intersection after vehicle i, it should maintain a safe following distance from vehicle i:

$$t_j' - t_i' \geq \frac{(l_c + \Delta d)}{v} \cdot \vartheta_{ij} + (\vartheta_{ij} - 1) \cdot M, \quad \forall i,j \in C, \quad i \neq j \tag{8}$$

$$t_j' - t_i' \leq \frac{(l_c + \Delta d)}{v} \cdot (\vartheta_{ij} - 1) + \vartheta_{ij} \cdot M, \quad \forall i,j \in C, \quad i \neq j \tag{9}$$

Vehicle kinematic constraints. Vehicles entering the intersection optimisation zone should comply with the kinematic constraints on speed and acceleration:

$$v_t^c \in [v_{min}^c, \ v_{max}^c], \quad \forall t \in T, \quad t \leq t_c' \tag{10}$$

$$a_t^c \in [a_{min}^c,\ a_{max}^c],\ \forall t \in T,\ t \le t_c' \tag{11}$$

Length of the optimisation zone. To ensure that vehicles can adjust to the specified speed before entering the intersection, the length of the optimisation zone should satisfy the following requirements:

$$2a_{max}^c \cdot L_{adjust} \ge v_m^2 - v_{c0}^2,\ \forall c \in C \tag{12}$$

Time cycle. Assuming a long time cycle T, all vehicles could leave the intersection before the time cycle completes:

$$x_T^c - L_{r^c} \ge 0 \tag{13}$$

Vehicle and pedestrian travel time. For vehicles entering the intersection, the relationship between the travel distance along a fixed path and the time is expressed in *Equation 14*:

$$x_t^c = (t - t_c') \cdot v_m,\ \forall t \in T,\ \forall c \in C \tag{14}$$

The exit time t_c^+ for the vehicle leaving the intersection is determined by the entry time t_c', the vehicle's speed v_m within the intersection and the length of its travel path, as shown in *Equation 15*:

$$t_c^+ = \frac{l_c^r}{v_m} + t_c',\ \forall c \in C,\ \forall r \in R \tag{15}$$

The time at which a vehicle reaches the lower and upper boundaries of a conflict zone on its path is given by *Equations 16 and 17*:

$$\underline{t}_c^{b,r} = \frac{\underline{\mu}_c^{b,r}}{v_m} + t_c',\ \forall c \in C,\ \forall r \in R,\ \forall b \in B^{r^c} \tag{16}$$

$$\overline{t}_c^{b,r} = \frac{\overline{\mu}_c^{b,r}}{v_m} + t_c',\ \forall c \in C,\ \forall r \in R,\ \forall b \in B^{r^c} \tag{17}$$

The time at which a vehicle reaches the lower and upper boundaries of the conflict zone between its path and the pedestrian crosswalks is given by *Equations 18 and 19*:

$$\underline{t}_c^{s,r} = \frac{\underline{\mu}_c^{s,r}}{v_m} + t_c',\ \forall c \in C,\ \forall r \in R,\ \forall s \in S^{r^c} \tag{18}$$

$$\overline{t}_c^{s,r} = \frac{\overline{\mu}_c^{s,r}}{v_m} + t_c',\ \forall c \in C,\ \forall r \in R,\ \forall s \in S^{r^c} \tag{19}$$

The entry time of the vehicle should not be earlier than the time it arrives at the intersection. Therefore, the following constraint is added:

$$t_c' \ge t_c^-,\ \forall c \in C \tag{20}$$

4.3 Collision avoidance

To separate potential conflicts within the intersection, collision avoidance constraints should be added. These constraints can be divided into vehicle-to-vehicle and vehicle-to-pedestrian collision avoidance.

Vehicle-to-vehicle collision avoidance

One conflict zone can be occupied by no more than one vehicle at any given time. To ensure that, it is necessary to assess the conflict zone occupancy time for all vehicles. Two binary variables, $y_{c,t}^b$ and $y_{c,t}'^b$ are introduced to model whether a vehicle is in the conflict zone [11]. The variable $y_{c,t}^b$ represents whether a vehicle has entered a conflict zone $b \in B^{r^c}$ along its path. If the vehicle has entered the conflict zone, $y_{c,t}^b = 1$. Otherwise, $y_{c,t}^b = 0$. Similarly, $y_{c,t}'^b$ represents whether a vehicle that has entered the conflict zone $b \in B^{r^c}$ has

left it. If the vehicle has not yet exited the conflict zone, $y'^{b}_{c,t} = 1$. Otherwise, $y'^{b}_{c,t} = 0$. These relationships can be described as follows:

$$y^{b}_{c,t} \geq (t - \underline{t}^{b,r}_{c}) \times \varepsilon,\ \forall t \in T,\ \forall c \in C,\ \forall b \in B^{r^c} \tag{21}$$

$$y^{b}_{c,t} - 1 \leq (t - \underline{t}^{b,r}_{c}) \times \varepsilon,\ \forall t \in T,\ \forall c \in C,\ \forall b \in B^{r^c} \tag{22}$$

$$y'^{b}_{c,t} \geq (\bar{t}^{b,r}_{c} - t) \times \varepsilon,\ \forall t \in T,\ \forall c \in C,\ \forall b \in B^{r^c} \tag{23}$$

$$y'^{b}_{c,t} - 1 \leq (\bar{t}^{b,r}_{c} - t) \times \varepsilon,\ \forall t \in T,\ \forall c \in C,\ \forall b \in B^{r^c} \tag{24}$$

The following conflict zone occupancy constraint is added. It can be easily proven that the constraint is not satisfied only if the variables $y^{b}_{c,t}$, $y'^{b}_{c,t}$, $y^{b}_{c',t}$, and $y'^{b}_{c',t}$ all equal 1, meaning that there are two vehicles in the same conflict zone at the same time:

$$y^{b}_{c,t} + y'^{b}_{c,t} + y^{b}_{c',t} + y'^{b}_{c',t} \leq 3,\ \forall c, c' \in C,\ \forall t \in T,\ r^c \neq r^{c'},\ \forall b \in B^{r^c} \cap B^{r^{c'}} \tag{25}$$

Vehicle-to-pedestrian collision avoidance

To solve the potential conflicts between vehicles and pedestrian crosswalks, two binary variables, $z^{s}_{c,t}$ and $z'^{s}_{c,t}$ are introduced. The variable $z^{s}_{c,t}$ indicates whether a vehicle has entered the conflict zone between its path and the crosswalk. When a vehicle enters any conflict zone $s \in S^{r^c}$ on its path, $z^{s}_{c,t} = 1$. Otherwise, $z^{s}_{c,t} = 0$. The variable $z'^{s}_{c,t}$ is used to determine whether the vehicle has left the conflict zone. If the vehicle has not left the conflict zone $s \in S^{r^c}$, then $z'^{s}_{c,t} = 1$. Otherwise, $z'^{s}_{c,t} = 0$. The specific formulas are as follows:

$$z^{s}_{c,t} \geq (t - \underline{t}^{s,r}_{c}) \times \varepsilon,\ \forall t \in T,\ \forall c \in C,\ \forall s \in S^{r^c} \tag{26}$$

$$z^{s}_{c,t} - 1 \leq (t - \underline{t}^{s,r}_{c}) \times \varepsilon,\ \forall t \in T,\ \forall c \in C,\ \forall s \in S^{r^c} \tag{27}$$

$$z'^{s}_{c,t} \geq (\bar{t}^{s,r}_{c} - t) \times \varepsilon,\ \forall t \in T,\ \forall c \in C,\ \forall s \in S^{r^c} \tag{28}$$

$$z'^{s}_{c,t} - 1 \leq (\bar{t}^{s,r}_{c} - t) \times \varepsilon,\ \forall t \in T,\ \forall c \in C,\ \forall s \in S^{r^c} \tag{29}$$

Similarly, two binary variables, $z^{s}_{p,t}$ and $z'^{s}_{p,t}$ are introduced. The variable $z^{s}_{p,t}$ determines whether the pedestrian green phase at crosswalk s is activated at time t. If the phase is activated, $z^{s}_{p,t} = 1$. Otherwise, $z^{s}_{p,t} = 0$. The variable $z'^{s}_{p,t}$ indicates whether the phase has ended. If the phase is still active at time t, $z'^{s}_{p,t} = 1$. Otherwise, $z'^{s}_{p,t} = 0$.

$$z^{s}_{p,t} \geq (t - t'_{p}) \times \varepsilon,\ \forall t \in T,\ \forall p \in P,\ \forall s \in S^{r^p} \tag{30}$$

$$z^{s}_{p,t} - 1 \leq (t - t'_{p}) \times \varepsilon,\ \forall t \in T,\ \forall p \in P,\ \forall s \in S^{r^p} \tag{31}$$

$$z'^{s}_{p,t} \geq (t'_{p} + t_{p} - t) \times \varepsilon,\ \forall t \in T,\ \forall p \in P,\ \forall s \in S^{r^p} \tag{32}$$

$$z'^{s}_{p,t} - 1 \leq (t'_{p} + t_{p} - t) \times \varepsilon,\ \forall t \in T,\ \forall p \in P,\ \forall s \in S^{r^p} \tag{33}$$

The conflict zone occupancy constraint is shown in *Equation 34*. It can be proven that this constraint is satisfied when the variables $z^{s}_{c,t}$, $z'^{s}_{c,t}$, $z^{s}_{p,t}$ and $z'^{s}_{p,t}$ equal 1. In other words, the constraint is not satisfied when the period during which a vehicle occupies the conflict zone between the crosswalk r^p and the path r^c conflicts with the pedestrian signal phase.

$$z^{s}_{c,t} + z'^{s}_{c,t} + z^{s}_{p,t} + z'^{s}_{p,t} \leq 3,\ \forall c \in C,\ \forall p \in P,\ \forall t \in T,\ \forall s \in S^{r^c} \cap S^{r^p} \tag{34}$$

4.4 Objective function

The objective function is to minimise the total delay of vehicles and pedestrians. Vehicle delay is defined as the difference between the minimum time required for a vehicle to pass through the intersection at free-flow speed and the actual time taken. As vehicle speed is constant at free-flow speed, the vehicle delay is equivalent to the time gap between the time the vehicle is permitted to enter the intersection and the arrival time at the intersection. Pedestrian delay is defined as the difference between the pedestrian arrival time and the allowed entry time at the intersection. The objective function is expressed as follows:

$$min\ Delay = min \sum_{c=1}^{C} (t_c^+ - t_c^- - t_c^{min}) + min \sum_{p=1}^{P} (t'_{p_0} - t_{p_0}^- + t'_{p_1} - t_{p_1}^-),\ \forall c \in C,\ \forall p \in P \tag{35}$$

By combining objective *Equation 35* with constraints *Equations 1–34*, the optimal entry time t_c' for vehicles into the intersection, the pedestrian green phase release time t'_{p_0} and its duration t_{p_0} for the first stage, the pedestrian green phase release time t'_{p_1} and its duration t_{p_1} for the second stage, along with the total delay, can be obtained.

5. NUMERICAL EXPERIMENTS

In this section, the effectiveness of the proposed pedestrian crossing control method is verified. The average vehicle delay and average pedestrian delay are used as indicators to compare the performance. In the comparative analysis of different control strategies, the signal control strategy for pedestrian crossing in one go proposed in the study of Niels et al. [19] is selected for comparison. To ensure the fairness of the numerical results, its reservation strategy based on FCFS rules is replaced by the proposed control strategy based on conflict separation.

5.1 Numerical settings

The conventional four-arm intersection shown in *Figure 1* is taken as an example. Each arm has six lanes. The lane width is set to 3 metres. The length of the optimisation zone is 100 metres. The crosswalk in each approach is set as 3 metres wide and 18 metres long. Vehicle and pedestrian arrivals follow the Poisson distribution [30]. In each traffic scenario, vehicle and pedestrian arrivals are randomly generated three times [9]. The mean value of the three experiments' average delay is chosen as the final result. The vehicle demand for each lane ranges from 400 to 800 pcu/h in increments of 200 pcu/h, which covers low, medium and high-level demands. The traffic demand at each approach is evenly distributed among left-turn, straight and right-turn movements. The pedestrian demand for each waiting area ranges from 100 to 400 ped/h in increments of 100 ped/h to represent low, medium and high-level demands. The pedestrian crossing phase is triggered as follows. Pedestrian arrival time is recorded upon the arrival of the first pedestrian in the waiting area. Subsequently, pedestrian arrivals are recorded. Once the number of pedestrians in the waiting area reaches five, a pedestrian crossing request is sent to the intersection's central controller. Additionally, the first pedestrian's waiting time should not exceed 30 seconds. Even though the pedestrian arrival number has not reached five, a crossing request should still be generated and sent to the central intersection controller if the waiting time for the first pedestrian is up to 30 s.

The experiments are solved by a Cplex mathematical programming solver and conducted on a desktop computer with Win-11 64-bit operating system, Intel(R) Core(TM) i7-12700H CPU 2.30 GHz, and 16.0 GB RAM GeForce.

5.2 Results and analysis

A comparative comparison of the two-stage PCISC method and the signal control method for pedestrian crossing in one go is conducted in this section. The summarised delay time for vehicles and pedestrians in each of the demand scenarios for both crossing in one go and two-stage crossing methods is shown in Figure *8*. The results indicate that the two-stage PCISC model can reduce total delays under all circumstances, with an average delay reduction of 40.86%. In the following part, we will divide the analysis by different control methods and traffic scenarios to compare the simulation results of vehicle delays and pedestrian delays separately.

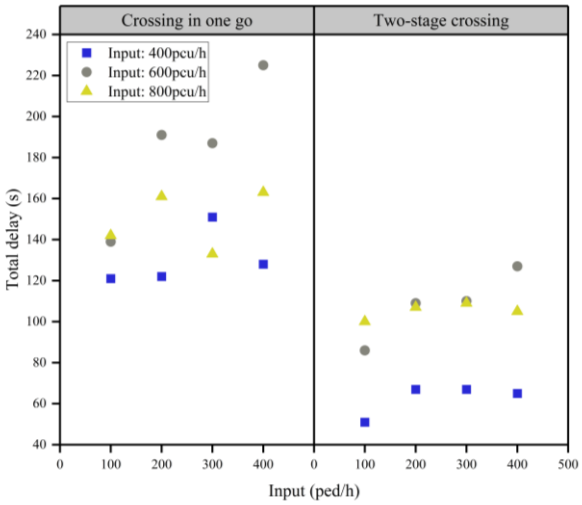

Figure 8 – Total delay for vehicles and pedestrians in each of the demand scenarios

Comparison of different control methods

The pedestrian crossing delays of two-stage crossing and crossing in one go are shown in *Figure 9*. The results indicate that the two-stage PCISC model consistently results in lower average pedestrian crossing delays compared to the signal control model for pedestrian crossing in one go, with an average delay reduction of 48.08%. Specifically, when pedestrian demand is 400 ped/h and vehicle demand is 800 pcu/h, the two-stage PCISC method achieves the greatest reduction of 72.73% in average pedestrian crossing delay.

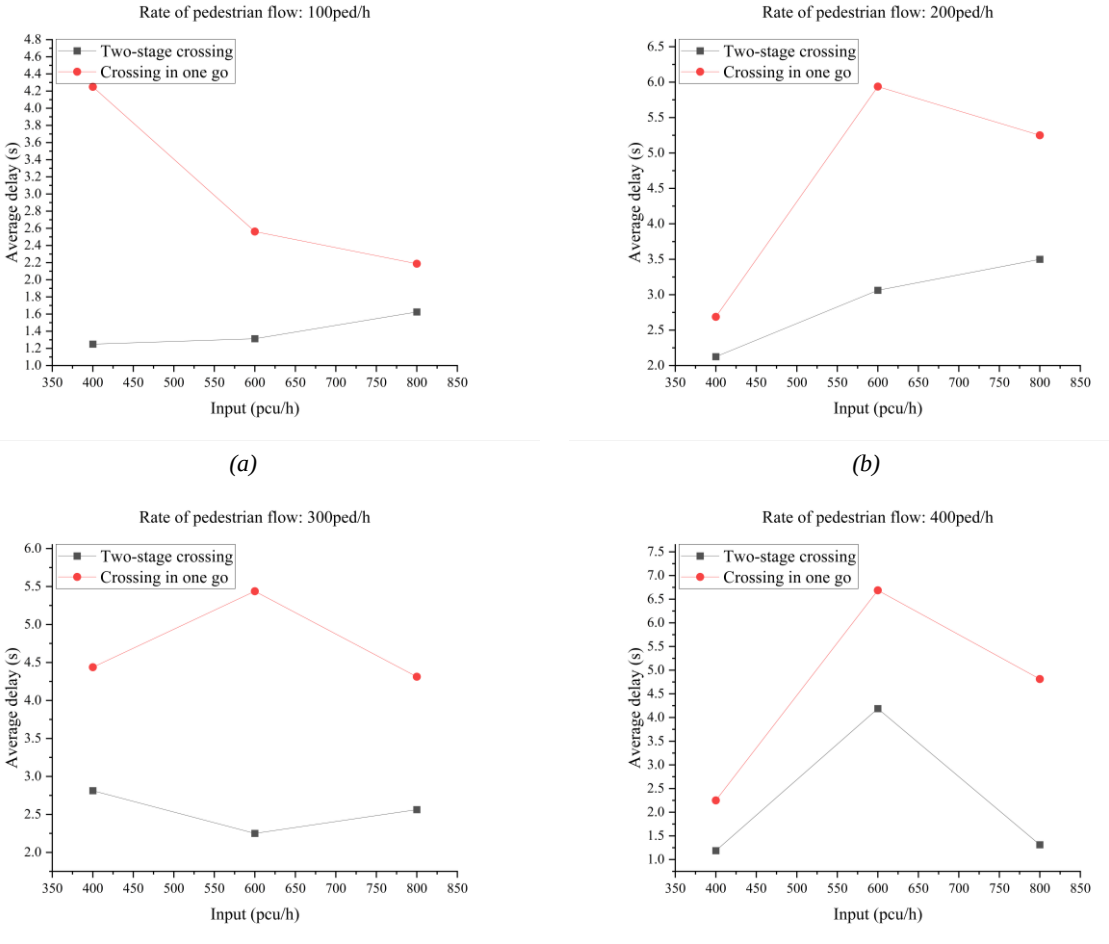

(a) *(b)*

(c) *(d)*

Figure 9 – Average delay of pedestrian crossing: a) 100 ped/h of pedestrian flow; b) 200 ped/h of pedestrian flow; c) 300 ped/h of pedestrian flow; d) 400 ped/h of pedestrian flow

The vehicle delays are shown in *Figure 10*. It is evident that, compared to scenarios only considering vehicle demands, pedestrian crossing increases vehicle delays. In particular, the two-stage PCISC model increases vehicle delays by an average of 292.52%, whereas the signal control model for pedestrian crossing in one go increases vehicle delays by an average of 697.49%. The two-stage PCISC model usually results in lower vehicle delays, with an average delay reduction of 35.77%. Specifically, when pedestrian demand is 300 ped/h and vehicle demand is 400 pcu/h, the two-stage PCISC method achieves the greatest reduction of 72.50% in average vehicle delays. At the same time, as pedestrian and vehicle demand simultaneously increases, the advantage of the two-stage PCISC in reducing average vehicle delay becomes progressively smaller compared to the signal control for pedestrian crossing in one go. When pedestrian demand is 300 ped/h and vehicle demand is 800 pcu/h, the average vehicle delay for the two-stage PCISC is 6.25% higher. However, it is important to note that in this scenario, the two-stage PCISC still achieves a 40.58% reduction in average pedestrian crossing delay compared to the signal control method for pedestrian crossing in one go.

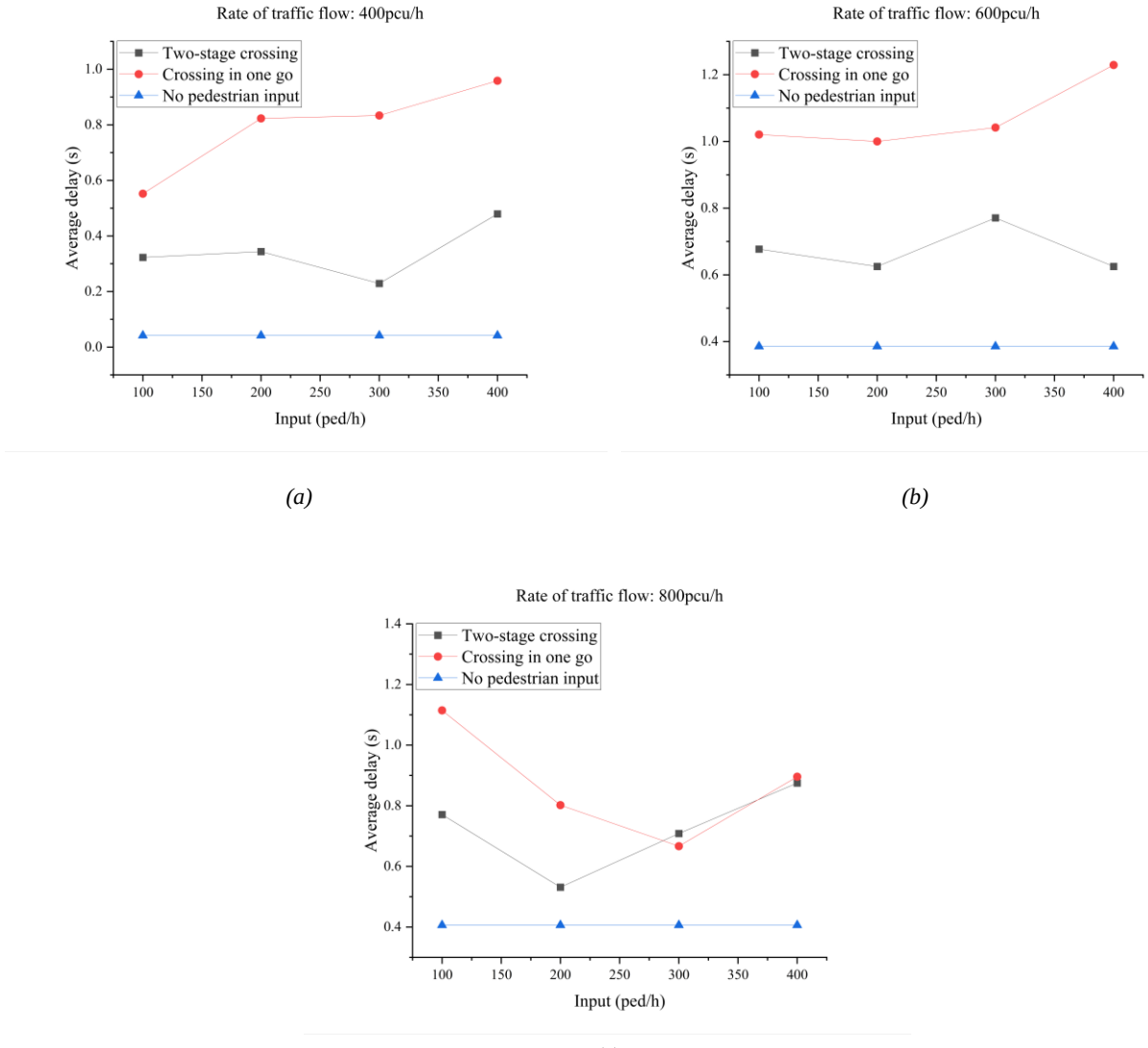

Figure 10 – Average delay of vehicles: a) 400 pcu/h of traffic flow; b) 600 pcu/h of traffic flow; c) 800 pcu/h of traffic flow

Comparison of different traffic demands

The comparison of vehicle and pedestrian crossing delays across varying demands is illustrated in *Figure 11*. The delays exhibit a similar trend under both control methods. As vehicle or pedestrian demands increase, the overall delays for vehicles and pedestrians tend to increase. Moreover, the average pedestrian crossing delay remains consistently higher than the vehicle delay. This is because the conflict-free gaps needed for pedestrians to cross are larger compared to those for vehicles.

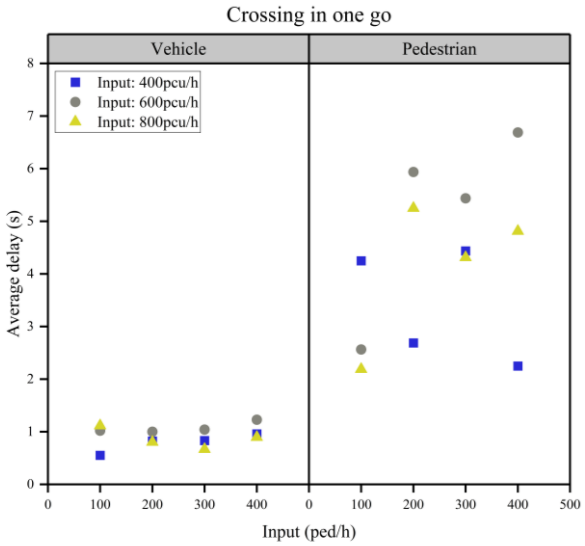

(a)

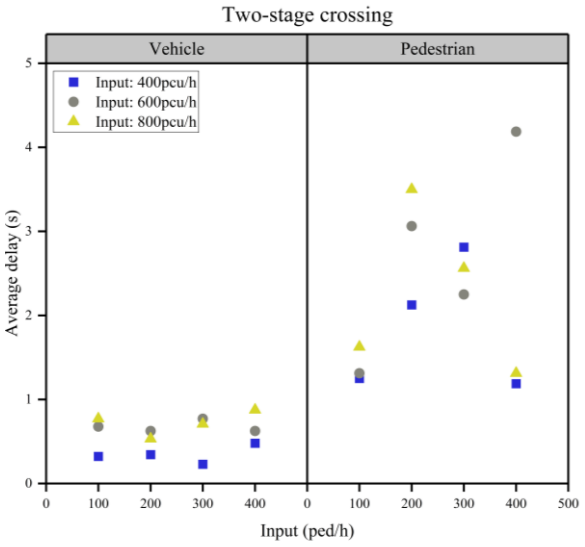

(b)

Figure 11 – Average delay of pedestrians and vehicles: a) Crossing in one go; b) Two-stage crossing

Pedestrian signal timing scheme

Taking the west approach as an example, the intersection control results are analysed with the demand of vehicles and pedestrians being 600 pcu/h and 300 ped/h, respectively. *Figures 12a and 12b* show the pedestrian crossing inductive signal timing scheme under the two-stage crossing and crossing in one go. From *Figure 12a*, it can be seen that the first pedestrian crossing demand appears on side a at 15 seconds. Then the first stage crossing phase turns green and lasts for 11 seconds. During this phase, pedestrians cross and reach the refuge island c. Then, the second-stage crossing phase turns green and lasts for 11 seconds, allowing pedestrians to cross without waiting. At 30 seconds, a pedestrian crossing demand p' appears on side b. However, the remaining green phase is insufficient to meet the minimum crossing time requirement. The pedestrian has to wait for the next green phase starting at 44 seconds. This phase also lasts for 11 seconds, enabling pedestrians p' on the side b to reach the refuge island c. Then, the second-stage crossing phase turns green and lasts for 22 seconds, allowing pedestrians to cross directly and leave the intersection at 66 seconds. Note that the second-stage crossing phase for pedestrians p' is the same as the first-stage crossing phase for pedestrians p,

while the first-stage crossing phase for pedestrians p' is the same as the second-stage crossing phase for pedestrians p.

Figure 12b shows that the first green phase at the west approach occurs at 26 seconds according to the signal control model for pedestrians crossing in one go. When a pedestrian crossing demand first appears on side a at 15 seconds, the signal phase is red. The pedestrian is required to wait for 11 seconds until the green phase is activated. This green phase lasts for 22 seconds. At 30 seconds, a pedestrian crossing demand occurs on side b. Since the pedestrian crossing phase is green with sufficient remaining time to meet the minimum crossing time requirement, the pedestrian can cross without waiting.

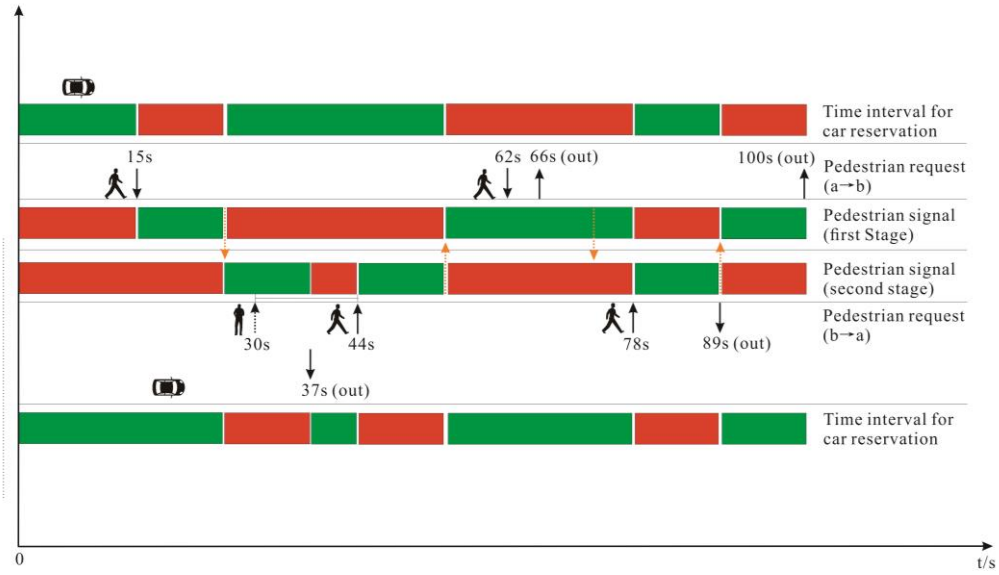

(a)

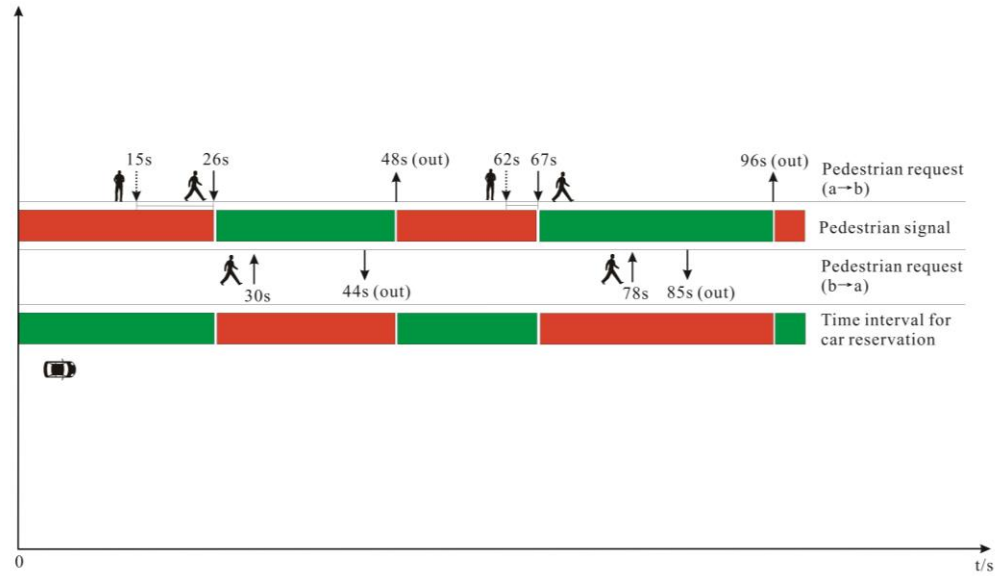

(b)

Figure 12 – Pedestrian crossing phase at the west approach: a) Two-stage crossing; b) Crossing in one go

By comparing the vehicle traversable gaps in *Figures 12a and 12b*, it is evident that the two-stage PCISC method provides more and more dispersed vehicle traversable gaps compared to the method for pedestrian crossing in one go. Under the two-stage PCISC method, the exit direction of the west approach has vehicle traversable gaps at 0–14 seconds, 26–54 seconds and 78–88 seconds, totalling 52 seconds. In the entry direction,

the vehicle traversable gaps occur at 0–25 seconds, 37–43 seconds, 55–77 seconds and 89–100 seconds, totalling 64 seconds. In contrast, under the signal control method for pedestrian crossing in one go, the vehicle traversable gaps in both entry and exit directions of the west approach occur at 0–25 seconds, 48–66 seconds and 96–100 seconds, totalling 47 seconds.

6. CONCLUSION

This paper focuses on the problem of pedestrian crossing under the AIM model and proposes a new two-stage PCISC method for pedestrian crossing. Firstly, the pedestrian walking characteristics are investigated to establish the phase-switching logic of the pedestrian signal, and the trajectory equations of CAVs at intersections are established. Then, a MILP model with the constraints of separating the occupancy time of the conflict areas inside the intersection between vehicles and pedestrians is proposed. The numerical result shows that the proposed model for AIM is feasible. To verify the effectiveness of the proposed method, the performance of the proposed method with the signal control strategy for pedestrian crossing in one go is compared under different traffic demands. The comparison result shows that the proposed method outperforms the signal control for pedestrians crossing in one go in reducing average delay.

The proposed method in this paper is more flexible compared to the signal control strategy for pedestrian crossing in one go. Besides, the proposed model reduces the right-of-way disruption of CAVs caused by pedestrians. This can be achieved by reducing the pedestrian signals' occupancy time. The model decreases overall intersection delays and adapts well to changes in real-time intersection demands. At the same time, this method still has some limitations. For example, the objective function assigns the same weight to vehicle and pedestrian delays. However, the pedestrian priority or vehicle priority under different traffic scenarios should be considered to achieve a more reasonable allocation of spatiotemporal resources at intersections. In addition, due to the large computational load of solving MILP models, it is often challenging to meet the real-time solving requirements. Methods should be considered to accelerate the solution process in the future.

ACKNOWLEDGEMENTS

This research was supported by the National Natural Science Foundation of China via project No. 72474184 and Sichuan Science and Technology Program No. MZGC20240036.

REFERENCES

[1] Dresner KM, Stone P. A multiagent approach to autonomous intersection management. *Articial Intelligence Research*. 2008;31(3):591-656. DOI: 10.1613/jair.2502.

[2] Li L, Wang FY. Cooperative driving at blind crossings using intervehicle communication. *IEEE Transactions on Vehicular Technology*. 2006;55(6):1712-1724. DOI: 10.1109/TVT.2006.878730.

[3] Ahmane M, et al. Modeling and controlling an isolated urban intersection based on cooperative vehicles. *Transportation Research Part C: Emerging Technologies*. 2013;28(3):44-62. DOI: 10.1016/j.trc.2012.11.004.

[4] Carlino D, Boyles SD, Stone P. Auction-based autonomous intersection management. *Proceedings of the 16th IEEE International Conference on Intelligent Transportation Systems, 6-9 Oct. 2013, Hague, Netherlands*. 2013. p. 529-534. DOI: 10.1109/ITSC.2013.6728285.

[5] Chen X, et al. A nearly throughput-maximum knotted intersection design and control for connected and automated vehicles. *Transportation research part B: methodological*. 2023;171:44-79. DOI: 10.1016/j.trb.2023.03.005.

[6] Lee J, Park B. Development and evaluation of a cooperative vehicles environment. *IEEE Transactions on Intelligent Transportation Systems*. 2012;13(1):81-90. DOI: 10.1109/TITS.2011.2178836.

[7] Zhu F, Ukkusuri SV. A linear programming formulation for autonomous intersection control within a dynamic traffic assignment and connected vehicle environment. *Transportation Research Part C*. 2015;55:363-378. DOI: 10.1016/j.trc.2015.01.006.

[8] Muller ER, Carlson RC, Junior WK. Intersection control for automated vehicles with MILP. *IFAC PapersOnLine*. 2016;49(3):37-42. DOI: 10.1016/j.ifacol.2016.07.007.

[9] Levin MW, Rey D. Conflict-point formulation of intersection control for autonomous vehicles. *Transportation Research Part C: Emerging Technologies*. 2017;85:528-547. DOI: 10.1016/j.trc.2017.09.025.

[10] Fayazi SA, Vahidi A. Mixed integer linear programming for optimal scheduling of autonomous vehicle intersection crossing. *IEEE Transactions on Intelligent Vehicles*. 2018;3(3):287-299. DOI: 10.1109/TIV.2018.2843163.

[11] Lu G, et al. Are autonomous vehicles better off without signals at intersections? A comparative computational study. *Transportation Research Part B: Methodological*. 2022;155:26–46. DOI: 10.1016/j.trb.2021.10.012.

[12] Chen X, et al. Improved reservation-based method with controllable gap strategy for vehicle coordination at non-signalized intersections. *Physica A: Statistical Mechanics and its Applications*. 2022;604(1):127953. DOI: 10.1016/j.physa.2022.127953.

[13] Deng Z, et al. Cooperative platoon formation of connected and autonomous vehicles: Toward efficient merging coordination at unsignalized intersections. *IEEE Transactions on Intelligent Transportation Systems.* 2023;24(5): 5625-5639. DOI: 10.1109/TITS.2023.3235774.

[14] Hao R, et al. Managing connected and automated vehicles with flexible routing at "lane-allocation-free" intersections. *Transportation Research Part C: Emerging Technologies*. 2023;152:104152. DOI: 10.1016/j.trc.2023.104152.

[15] Amouzadi M, Orisatoki MO, Dizqah AM. Optimal lane-free crossing of cavs through intersections. *IEEE Transactions on Vehicular Technology.* 2022;72(2):1488-1500. DOI: 10.1109/TVT.2022.3207054.

[16] Hua B, et al. A novel intelligent intersection management scheme focusing on cooperative trajectory planning of connected automated vehicles. *IEEE Transactions on Intelligent Vehicles.* 2024. DOI: 10.1109/TIV.2024.3401146.

[17] Sun Q, et al. Reducing violation behaviors of pedestrians considering group interests of travelers at signalized crosswalk. *Physica A: Statistical Mechanics and its Applications*. 2022;594:127023. DOI: 10.1016/j.physa.2022.127023.

[18] Gupta S, Vasardani M, Winter S. Negotiation between vehicles and pedestrians for the right of way at intersections. *IEEE Transactions on Intelligent Transportation Systems*. 2019;20(3):888–899. DOI: 10.1109/TITS.2018.2836957.

[19] Niels T, et al. Smart intersection management for connected and automated vehicles and pedestrians. *2019 6th International Conference on Models and Technologies for Intelligent Transportation Systems (MT-ITS)*, 5-7 Jun. 2019, Cracow, Poland. 2019. p. 1-10. DOI: 10.1109/MTITS. 2019.8883362.

[20] Chen R, et al. Stability-based analysis of autonomous intersection management with pedestrians. *Transportation Research Part C: Emerging Technologies*. 2020;114:463–483. DOI: 10.1016/j.trc.2020.01.016.

[21] El Hamdani S, Benamar N, Younis M. A protocol for pedestrian crossing and increased vehicular flow in smart cities. *Journal of Intelligent Transportation Systems Technology Planning and Operations*. 2019;24(98):514–533. DOI: 10.1080/15472450.2019.1683451.

[22] Niels T, et al. Optimization-based intersection control for connected automated vehicles and pedestrians. *Transportation research record.* 2024;2678(2):135-152. DOI: 10.1177/03611981231172956.

[23] Cai P, He J, Li Y. Hybrid cooperative intersection management for connected automated vehicles and pedestrians. *Journal of Intelligent and Connected Vehicles.* 2023;6(2):91-101. DOI: 10.26599/JICV.2023.9210008.

[24] Mokhtari K, Wagner AR. Pedestrian collision avoidance for autonomous vehicles at unsignalized intersection using deep q-network. A*rXiv preprint ArXiv*. 2021;2105:00153. DOI: 10.48550/arXiv.2105.00153.

[25] Mokhtari K, Wagner AR. Safe deep q-network for autonomous vehicles at unsignalized intersection. *ArXiv preprint ArXiv*. 2021;2106.04561.. DOI: 10.48550/arXiv.2106.04561.

[26] Malcolm P, Bogenberger K. Lane-free intersection control for connected automated vehicles prioritizing vulnerable road users. *Transportation Research Part C: Emerging Technologies.* 2025;170:104918. DOI: 10.1016/j.trc.2024.104918.

[27] Wu W, et al. Autonomous intersection management with pedestrians crossing. *Transportation Research Part C: Emerging Technologies*. 2022;135:103521. DOI: 10.1016/j.trc.2021.103521.

[28] Jiang H, et al. Pedestrian shuttle service optimization for autonomous intersection management. *Transportation Research Part C: Emerging Technologies*. 2024;163:104623. DOI: 10.1016/j.trc.2024.104623.

[29] Transportation Research Board(TRB). *Highway capacity manual (HCM) 2000*. Washington, D C: National Research Council; 2000.

[30] Li L, Wang F. Cooperative driving at blind crossings using intervehicle communication. *IEEE Transactions on Vehicular Technology*. 2016;55(6):1712–1724. DOI: 10.1109/TVT.2006.878730.

张千宜，余欣睿，刘昱岗，唐李莹

自动驾驶交叉口行人两阶段感应式信号控制过街策略研究

摘要
在完全自动驾驶环境下，“无信号”的自主交叉口管理（AIM）已成为研究热点。然而，关于如何在自动驾驶环境下保障行人安全过街的研究仍然较少。本文提出了一种新颖的感应式信号控制框架，该框架综合考虑了行人和自动驾驶车辆（CAV）的需求。该框架包含两个步骤：第一步，建立适用于自动驾驶交叉口的行人两阶段感应信号控制过街模块；第二步，协同优化 CAV 的行驶轨迹与行人过街相位。研究通过建立基于冲突分离的混合整数线性规划（MILP）模型，确定行人过街信号相位方案和 CAV 进入交叉口的最佳时刻，以达到交叉口总延误最小。最后通过案例仿真结果验证本研究所提出的控制方法在不同车辆及行人流量场景下的控制效果。结果表明，在低中高流量场景下，行人二次过街感应式信号控制方法在减少车辆通行延误方面均优于行人一次过街感应信号控制模式。

关键词
自主交叉口管理；自动驾驶车辆；行人过街；混合整数线性规划